Third International Symposium on Marine Propulsors
smp'13, Launceston, Tasmania, Australia, May 2013

The Hydrodynamic Performance of Propellers with Trans-Velocity Sections in Inclined Shaft Conditions

Ching-Yeh Hsin[1], Shang-Sheng Chin[2], Kuan-Kai Chang[2], Ya-Lin Tsai[2], Jeng-Lih Hwang[3]

[1]Department of Systems Engineering and Naval Architecture, National Taiwan Ocean University, Keelung, Taiwan
[2]Ship and Ocean Industries R&D Center
[3]Department of Engineering Science and Ocean Engineering, National Taiwan University, Taipei, Taiwan

ABSTRACT

The hydrodynamic performance of propellers with the trans-velocity sections are presented in this paper. The trans-velocity section is developed for not only having a satisfactory performance, but also having consistent performance at different inflow speeds. The development of a design procedure for the trans-velocity section and propellers with trans-velocity sections are first presented. The viscous flow RANS method is used in the design procedure, and this design procedure can be also applied to a propeller with different types of foil sections. Two different designs are demonstrated in the paper, one is a propeller with only the trans-velocity section, and the other one is a propeller with both the trans-velocity section and a section especially developed for yachts. The numerical results of the hydrodynamic performance are compared to the experimental data, and the performances of these propellers at different inclined shaft angles are investigated. It is found that the propeller with hybrid sections has a better performance than the one with trans-velocity section only which suffers from a serious thrust loss in inclined shaft conditions. A pre-swirl stator is also designed for the purpose of improving the performance, and it is found to be effective.

Keywords

Trans-velocity section, Inclined shaft condition, Pre-swirl stator, propeller design, RANS

1 INTRODUCTION

The hydrodynamic performance of propellers with the trans-velocity sections are presented in this paper. The trans-velocity section is developed for not only having a satisfactory performance, but also having consistent performance at different inflow speeds. Conventional propellers are designed to operate without blade surface cavitation, and the trans-velocity section is designed to keep the same lift at different inflow speeds. There are many design methods of foil sections proposed by scholars, such as Henne (1985), Giles (1986), Hsin (1994) etc. In order to design propellers that can be operated efficiently at a range of speeds, some researchers have worked on the designs of propellers with new sections, for example, Eppler (1980), Scherer and Stairs (1994), Shen (1996), Kehr (2001), Black (2006) and Young and Shen (2007). In this paper, we will briefly describe the design methods of sections and propellers, and then both the numerical computations and experimental data are used to investigate the designs.

2 THE TRANS-VELOCITY SECTION

The design method of the trans-velocity section has been described by Hwang et al (2009, 2011), and the design method is based on Hsin (1994, 1998, 2000). A multi-objective optimization problem is solved by the Lagrange Multiplier method with a weighting function. The designed section has to satisfy the force requirements at different speeds. Therefore, we have the following objective functions and constraints:

$$\begin{cases} \min \quad C_D^k \\ \\ subject\ to \quad C_L^k - C_L^{k*} \geq 0 \end{cases} \qquad k = 1, 2, 3... \tag{1}$$

The index k indicates different design conditions. When optimizing the performance of a section in different conditions, we can use a slack variable s_k to convert the constraints to:

$$C_L^k - C_L^{k*} - s_k^2 = 0 \tag{2}$$

In order to optimize the foil performance in different conditions, we then introduce a weighting function w, and the Lagrangian of this optimization problem becomes:

$$L = \sum_{k=1}^{N} [w_k C_D^k + \lambda_k (C_L^k - C_L^{k*} - s_k^2)] \tag{3}$$

In equation (3), the weighting function w is given by the designers, and it is selected by judging the importance of each design condition. To solve this optimization problem, we have

$$\begin{aligned} &\nabla_V L = \sum_{k=1}^{N} [w_k \nabla_V C_D^k + \lambda_k \nabla_V C_L^k] = 0 \\ &2\lambda_k s_k = 0 \\ &C_L^k - C_L^{k*} - s_k^2 = 0 \end{aligned} \tag{4}$$

We can define:

$$G = \begin{bmatrix} \nabla_V L \\ 2\lambda_k s_k \\ C_L^k - C_L^{k*} - s_k^2 \end{bmatrix}, \qquad \vec{X} = \begin{bmatrix} \alpha \\ \vec{\lambda} \\ \vec{\gamma} \\ \vec{s} \end{bmatrix}$$

where $\vec{\gamma} = [\gamma_1, \gamma_1 ... \gamma_m]^T$ if there are m geometric parameters, $\vec{\lambda} = [\lambda_1, \lambda_1 ... \lambda_N]^T$ and $\vec{s} = [s_1, s_1 ... s_N]^T$ if there are N constraints (N design conditions). The section geometry can then be solved by solving the equation (4). The computation is carried out by viscous flow RANS method, and the detailed procedure can be seen in Hwang (2009, 2011). The designed geometry is shown in Fig. 1, and the pressure distributions of this section at different inflow speeds are shown in Fig. 2. From Fig. 2, one can see that the aft part of this section give the negative lift at 20 knots without cavitation, and this negative lift is eliminated due to cavitation at 30 knots. This is the main reason that the trans-velocity section can provide very similar lift at different speeds.

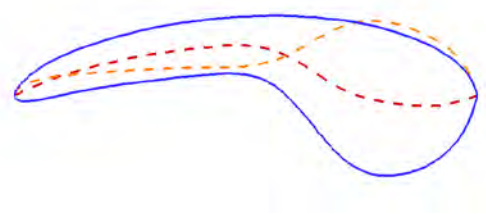

Fig. 1 The geometry of the trans-velocity section.

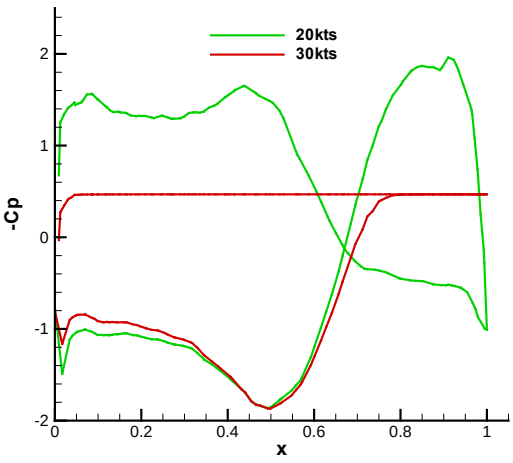

Fig. 2 The pressure distribution of the trans-velocity section at 20 knots and 30 knots.

3 VISCOUS FLOW COMPUTATIONS

The viscous flow RANS method is used to assist the design of a propeller with the trans-velocity sections. For viscous flow RANS computations, the commercial software FLUENT is used. It is a finite volume method based general-purpose CFD software. For steady inflow computations, the periodic boundary condition is used, and only one blade is needed to compute. However, for inclined shaft conditions, propeller blade encountered different angles of attack at different circumferential positions, and the unsteady flow computations have to be used. All blades have to be included in computational domain using sliding mesh shown in Fig. 3.

3.1 Boundary Conditions

The boundary conditions are set up as follows (Fig.3):

- Inlet/outlet boundary condition: The velocity inlet condition is set for the inlet boundary condition, and the pressure outlet boundary condition is set for the outlet.
- Wall boundary condition: The no-slip wall boundary condition is set for the propeller blade surface, and the grid interface is set with sliding meshes.

3.2 Grid Arrangement

Due to its high curvature surface of propeller geometry, a hybrid grid arrangement is used in this paper. The computational domain is composed of structured and unstructured grid systems. The unstructured grid system is used for the zones around the blades. The structured grid system is then adopted for the region outside the propeller since the geometry over there is relatively simple. A multi-block grid system generated from GRIDGEN is shown in Fig. 3.

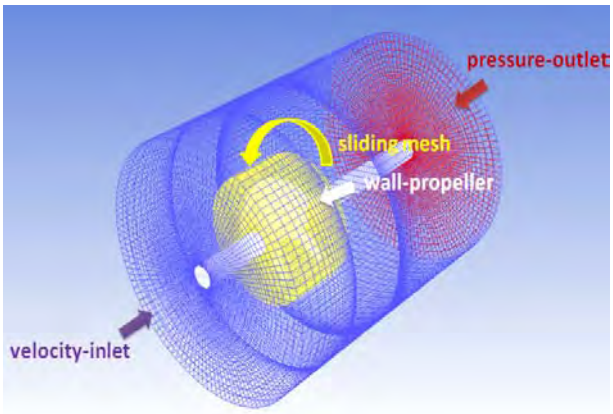

Fig. 3 The computational domain, boundary conditions and the grid arrangement of the RANS computations.

4 DESIGN OF PROPELLERS WITH TRANS-VELOCITY SECTIONS

Two different designs are demonstrated in the paper, one is a propeller with the trans-velocity section only, and the other one is a propeller with both the trans-velocity section and a section especially developed for high speed yachts (Kehr, 2001). A design procedure is developed for these designs, and experiments are carried out to verify the designs.

4.1 Propeller Design Procedure

The design procedure basically follows the procedure suggested by Kerwin (Kerwin , 1982).

(1) Select the basic propeller geometry parameters such as diameter, hub ratio, blade number and the initial guess distribution of chord length. Input basic

settings such as ship speed, engine speed (RPM) and torque.

(2) To obtain the optimum circulation distribution by using the lifting line method.

(3) To design the pitch and camber distributions by using the lifting surface program. A modified MIT-PBD-10 is used such that different sections can be used for one propeller.

(4) To evaluate the torque of designed propeller geometry by RANS to see if it meets the design requirement.

(5) If the RANS result is as expected, and the propeller design is obtained; otherwise, we have to return to the step (1) to adjust the input parameters till the designed geometry meet the requirement.

Some designs have been presented in the previous publications (Hwang et al, 2011). In this paper, two designs with TVP sections only and one design with hybrid sections will be presented.

4.2 Propellers with TVP Section Only

Based on the design procedure described above, a propeller with TVP section is designed, and it is named as "TVP1" propeller. The computational results are first verified to the experimental data. As described earlier, the commercial software FLUENT is used for the viscous flow computations, and the experiments are carried out at NTOU (National Taiwan Ocean University) medium size cavitation tunnel. Figs. 4 to 6 show the comparisons between the computational results and experimental data of TVP1 propeller performances at 20, 30 and 36 knots. Three different speeds are equivalent to the cavitation numbers 1.81, 0.80 and 0.55. For conventional propellers, the thrust and torque usually decrease as the cavitation happens. However, the characteristic of TVP propeller is that the thrust and torque increase as the cavitation happens. This is because the negative lift generated at the aft parts of the TVP section is eliminated as the cavitation happens. Figs. 7 to 9 show the computational pressure distribution and cavitation predictions compared with experimental data of TVP1 propeller. It is observed that the cavitation may initially appear on the face (pressure side) of propeller. When the ship speed increases, there may be cavitation occurring both on the face and back (suction side) in 30 to 36 knots. For the high speed, the cavity seems starting from the leading edge on the back, thus we observe from the computed cavity shape that the propeller is super-cavitating.

Although the efficiencies of TVP1 propeller are maintained over 0.63 from 20 to 36 knots in 0 degrees inclined shaft condition, the blade structural strength of TVP1 propeller is later found not sufficient. The second propeller with enough blade strength, TVP2, is then designed.

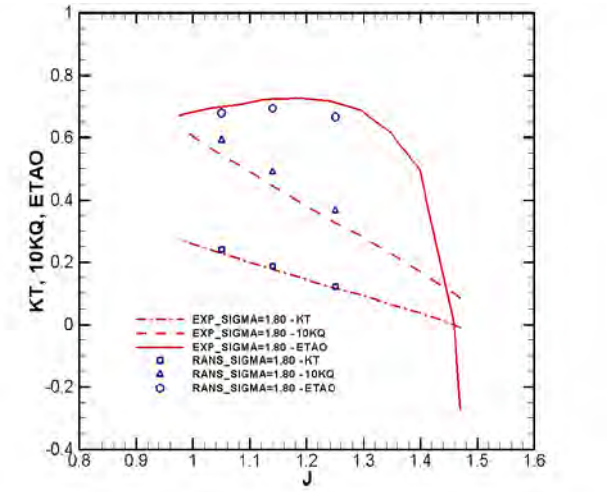

Fig. 4 The comparison between the computational results and experimental data of TVP1 performance at 20 knots.

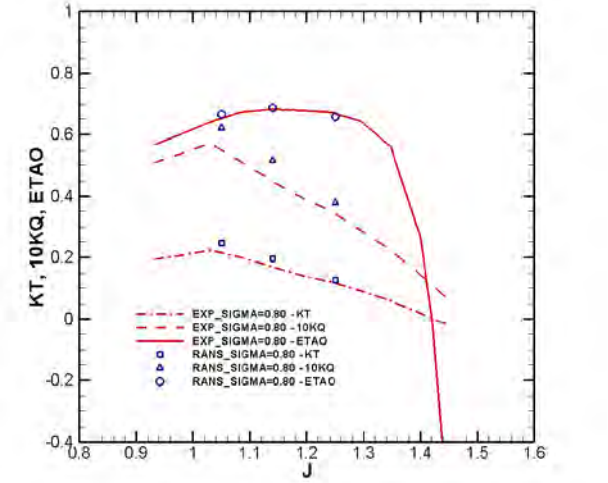

Fig. 5 The comparison between the computational results and experimental data of TVP1 performance at 30 knots.

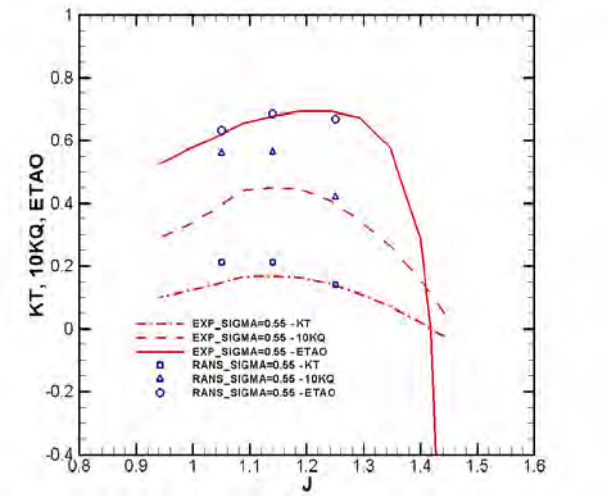

Fig. 6 The comparison between the computational results and experimental data of TVP1 performance at 36 knots.

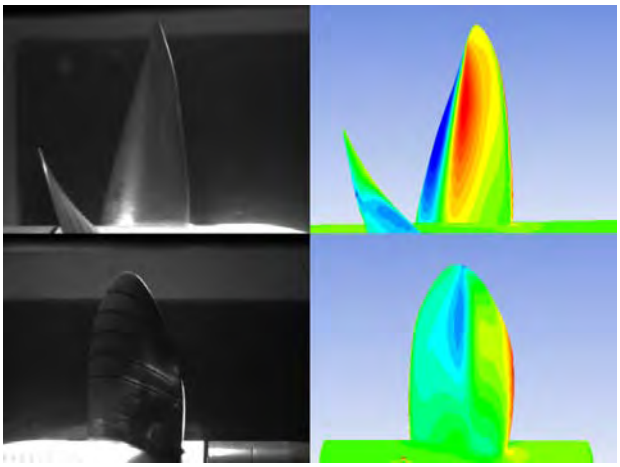

Fig. 7 The pressure distributions and cavitation predictions compared with experiments at 20 knots of TVP1 propeller. The upper figure shows the pressure side and lower figure shows the suction side.

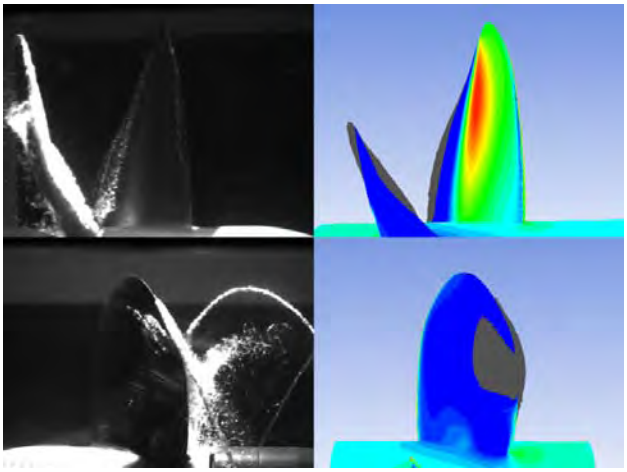

Fig. 8 The pressure distributions and cavitation predictions compared with experiments at 30 knots of TVP1 propeller. The upper figure shows the pressure side and lower figure shows the suction side.

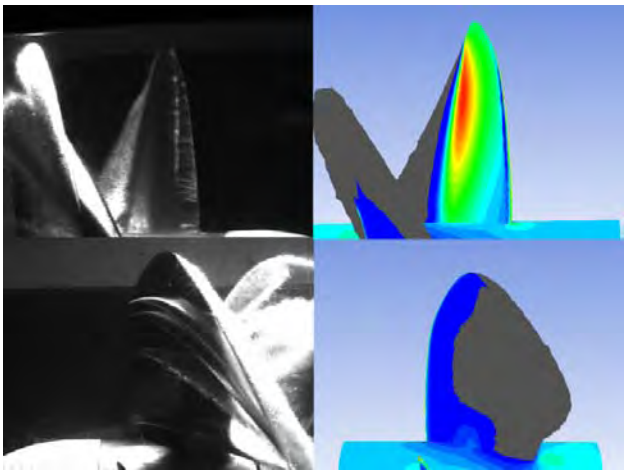

Fig. 9 The pressure distributions and cavitation predictions compared with experiment at 36 knots of TVP1 propeller. The upper figure shows the pressure side and lower figure shows the suction side.

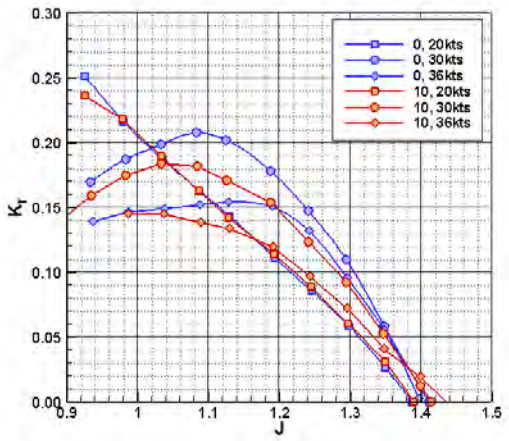

Fig. 10 The thrust coefficient (K_T) of the TVP2 propeller at different speeds and different inclined shaft angles. In the figure, "0, 20" means 0 degree inclined shaft angle, and ship speed 20 knots.

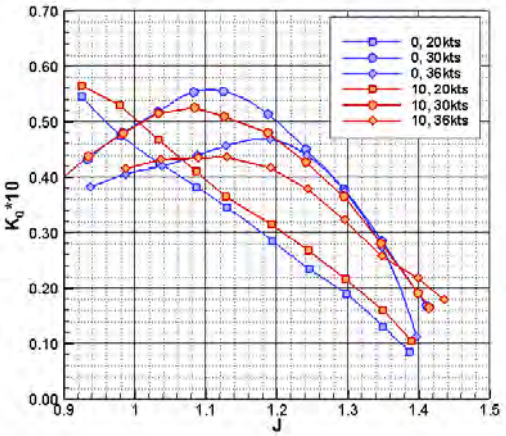

Fig. 11 The torque coefficient (K_Q) of the TVP2 propeller at different speeds and different inclined shaft angles.

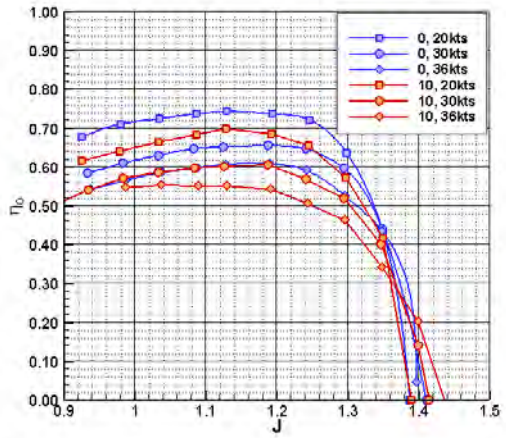

Fig. 12 The propeller efficiency (η_O) of the TVP2 propeller at different speeds and different inclined shaft angles.

Since most of the high speed propellers are installed with the inclined shaft; therefore, the performance of TVP2 propeller is investigated for the inclined shaft 0 and 10 degrees. The performance of TVP2 propeller at different speeds and different inclined shaft angles are shown in Fig. 10 to Fig. 12. One can see that as the inclined shaft angle increases from 0 degree to 10 degrees, both the thrust and torque drop, and these drops increase as the ship speed increases. On the other hand, the efficiencies drop with almost the same amount at different speeds.

4.3 Propellers with Hybrid Sections

The TVP2 propeller has a relatively poor performance at high speed and large inclined shaft angles. The poor performance at high speed indicates that TVP2 is not very well designed. The poor performance at large inclined shaft condition is because that as the propeller rotates to the starboard side, the negative angles of attack result in severe leading edge face cavitation for the TVP section. Since the face side near the leading edge provides most of the lift for TVP section (see Fig. 2), this will decrease the thrust a lot for a propeller with TVP section. To solve this problem, we decide to design a propeller with hybrid sections, and this propeller is named as “HB1” propeller. The "hybrid section propeller" here means that a propeller with different section geometries at different radii.

We have developed a design procedure for the hybrid section propeller, and it is as follows:

(1) The propeller is divided into three zones in the span-wise direction. A section especially for the high speed yachts, NS section, is adopted in the zone near the hub, and TVP section is adopted in the zone near the tip. The zone between these two is used to smoothly transfer the section geometry from NS section to TVP section.

(2) A modified MIT-PBD-10 for the hybrid section propeller is used to design the pitch and camber distributions based on the same loading distribution of TVP2 designed from the lifting line method.

(3) The propeller boundary element method is then used to compute the forces on the propeller, and the design loading distribution is scaled if the forces do not match the design goal. We will repeat step (2) and (3) until the design goal is reached.

(4) Go back to step (1) for another zone locations, and (2) and (3) will be iterated. We will select the best efficiency as our design.

(5) The RANS method is finally used to verify the forces on the propeller, and the design loading distribution will be scaled until the design goal is reached.

In the above design procedure, the boundary element method is mainly used to design the zone locations, and RANS method is used to make the final design. We finally get a design which it adopts the NS section from hub to r/R=0.5, and TVP sections from r/R=0.8 to the tip. We first verify the computational results, and Figs. 13 and 14 show the comparisons of thrusts and efficiencies between the computational results and experimental data of HB1 performance at 20, 30 and 36 knots for inclined shaft 0 degree. The comparison of torques show similar trend, and we will not show here. Figs. 15 and 16 present the comparisons of thrusts and efficiencies between the computational results and experimental data of HB1 performance at 20 and 30 knots for inclined shaft 10 degrees. Note that the experiment of 36 knots and inclined shaft 10 degrees case was not performed. From the comparisons, we can see that although the computational results and experiment data have some discrepancies, the trends are predicted correctly.

Figs. 17 to 19 show the performance of HB1 propeller from experiments, and one can see that the variations of thrusts and torques for different inclined shaft angles are much less than those of TVP2 propeller. Also the performances of HB1 propeller at all speeds are much better than TVP2 propeller.

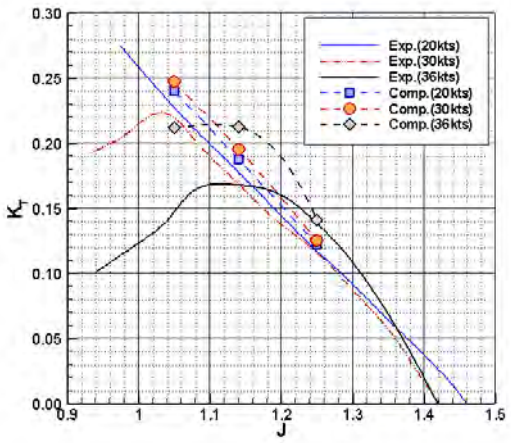

Fig. 13 The comparison of thrusts between the computational results and experimental data of HB1 performance at 20, 30 and 36 knots for inclined shaft 0 degree.

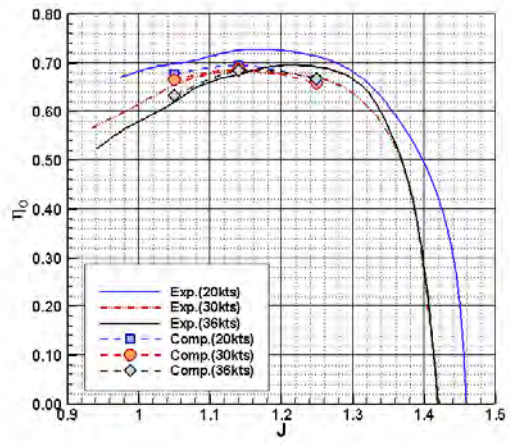

Fig. 14 The comparison of efficiencies between the computational results and experimental data of HB1 performance at 20, 30 and 36 knots for inclined shaft 0 degree.

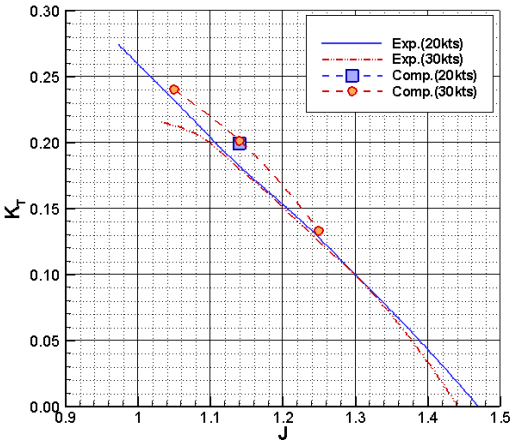

Fig. 15 The comparison of thrusts between the computational results and experimental data of HB1 performance at 20 and 30 knots for inclined shaft 10 degrees.

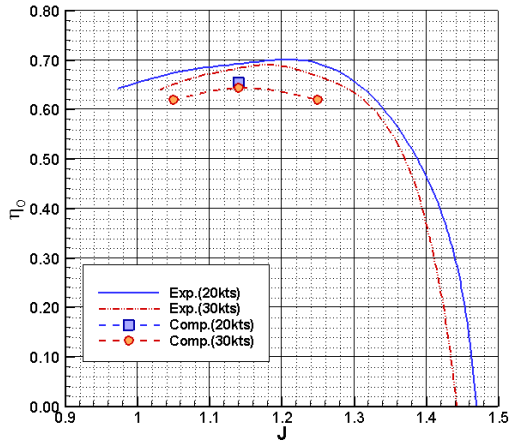

Fig. 16 The comparison of efficiencies between the computational results and experimental data of HB1 performance at 20 and 30 for inclined shaft 10 degrees.

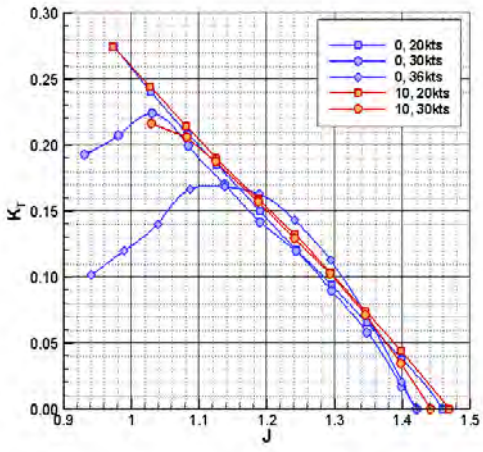

Fig. 17 The thrust coefficient (K_T) of the HB1 propeller at different speeds and different inclined shaft angles.

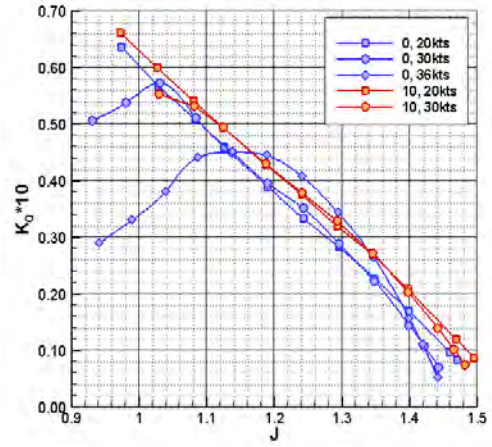

Fig. 18 The torque coefficient (K_Q) of the HB1 propeller at different speeds and different inclined shaft angles.

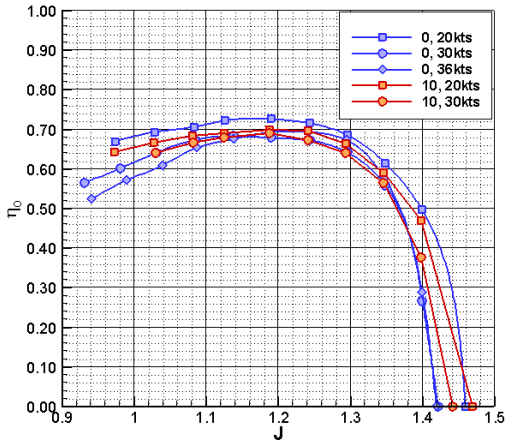

Fig. 19 The propeller efficiency (η_O) of the HB1 propeller at different speeds and different inclined shaft angles.

4.4 Propeller with the Pre-swirl Stator

In order to further improve the performance of HB1 propeller at inclined shaft conditions, a pre-swirl stator (PSS) is designed to install in front of the HB1 propeller. Fig. 20 shows the computer depictions of the pre-swirl stator with propeller. The pre-swirl stator is three bladed, and the blades are installed at 45, 90 and 135 degrees at port side. It is well known that the pre-swirl stator can decrease the angles of attack as the propeller rotates to the port side at inclined shaft condition, and it can also decrease the variations of the angles of attack circumferentially. This usually can increase the propeller efficiency and decrease the propeller unsteady forces.

Since the propeller geometry is fixed, a pre-swirl stator boundary element method is developed. A parametric design is carried out to the design the pitch angles (or angles of attack) of the stator blades.

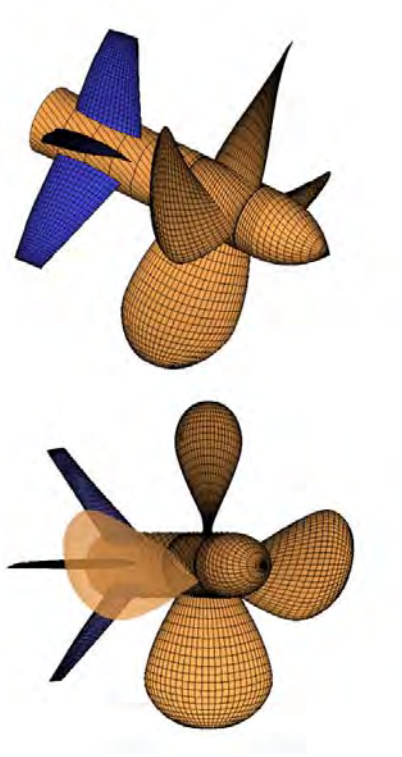

Fig. 20 The computer depictions of the pre-swirl stator with propeller. This pre-swirl stator is three bladed, and the blades are installed at 45, 90 and 135 degrees at port side.

The comparison of performances of TVP2 and HB1 propellers at 36 knots and 0 degree inclined shaft are shown in Fig. 21, and it is obvious that HB1 has a much better performance than TVP2. Fig. 22 shows the comparisons of performances of HB1 propeller and HB1 propeller with PSS at 36 knots and 8 degrees inclined shaft condition. Fig. 23 shows the comparisons of performances of TVP2, HB1 propellers and HB1 propeller with PSS at 30 knots and 10 degrees inclined shaft condition. Fig. 24 shows the comparisons of performances of TVP2 and HB1 propeller with PSS at 36 knots and 10 degrees inclined shaft condition. All the results show that at high speeds and large inclined shaft angles, HB1 propeller and HB1 propeller with PSS provide satisfactory performance. Due to the experiment setup, we cannot measure the force on the stator. Since the computational results predict the trends correctly in general, we will use the computational results to see the total performance of HB1+PSS and HB1 propellers. Table 1 shows the performances of these two propellers at 36 knots and 10 degrees inclined shaft for design J (1.14). The HB1 with PSS has gained 1.38% higher efficiency than the HB1 propeller alone.

5 CONCLUSIONS

The development of a design procedure for the trans-velocity section and propellers with trans-velocity sections are presented in this paper. In order to consider the viscous and cavitation effects, the viscous flow RANS method is used to assist the design. A design procedure for a propeller with different types of foil sections, that is, a hybrid section propeller is also presented in this paper. The computational results from the viscous flow RANS method are compared to the experimental data for both the TVP propeller and the hybrid section propeller, and the comparisons show that in general the computations can predict the trend correctly for different speeds and different inclined shaft angles.

Two different designs are demonstrated in the paper, one is a propeller with only the trans-velocity section, and the other one is a propeller with both the trans-velocity section and a section especially developed for yachts. It is found that the propeller with hybrid sections has a better performance than the one with trans-velocity section only which suffers from a serious thrust loss in inclined shaft conditions. The hybrid section propeller HB1 can deliver efficiencies more than 0.65 for 20 to 36 knots in 0 to 10 degrees inclined shaft conditions. A pre-swirl stator is designed for the purpose of improving the performance, and it is predicted that the pre-swirl stator can improve the efficiency by 1.38% at 36 knots and 10 degrees inclined shaft. More verifications of the designs of hybrid section propeller and pre-swirl stator should be carried out, and the applications of these propellers should be explored.

6 ACKNOWLEDGEMENTS

The authors would like to express their gratitude to Prof. Yi-Chih Chow and Mr. Yaw-Heui Lee for carrying out all the experiments at the National Taiwan Ocean University medium-size cavitation tunnel.

Table 1. The computational results of the total performance of HB1 propeller and HB1 propeller with PSS at 36 knots and inclined shaft 10 degrees (J =1.14).

	KT	KQ*10	η_O	η_O %
HB1	0.1811	0.5276	0.6228	
HB1+PSS	0.1983	0.5651	0.6366	+1.38%

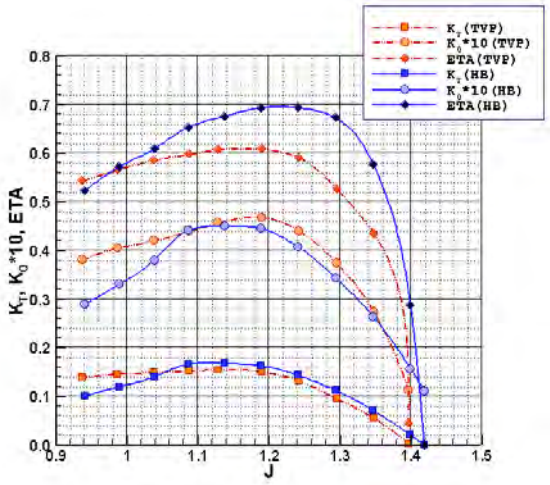

Fig. 21 The comparison of performances of TVP2 and HB1 propellers at 36 knots and 0 degree inclined shaft.

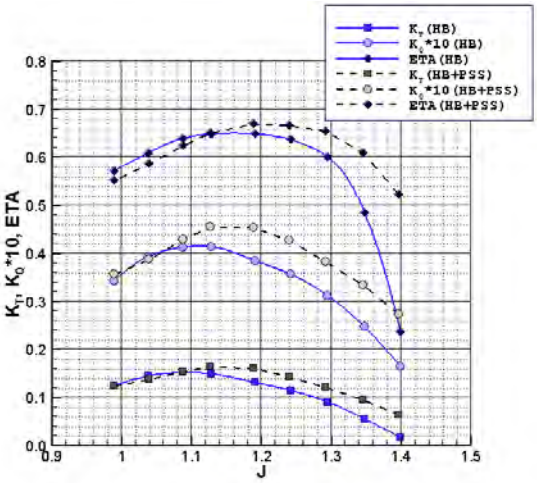

Fig. 22 The comparisons of performances of HB1 propeller and HB1 propeller with PSS at 36 knots and 8 degrees inclined shaft condition.

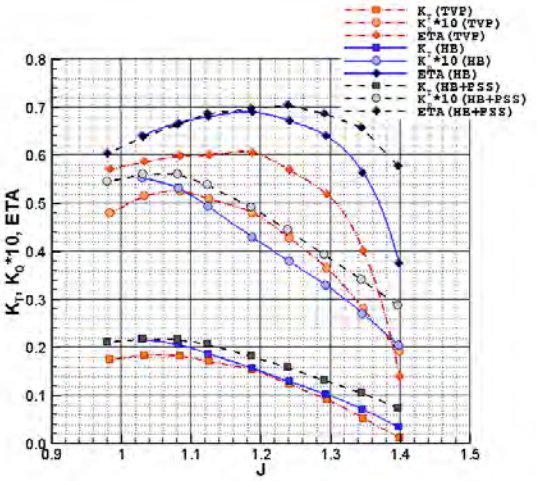

Fig. 23 The comparisons of performances of TVP2, HB1 propellers and HB1 propeller with PSS at 30 knots and 10 degrees inclined shaft condition.

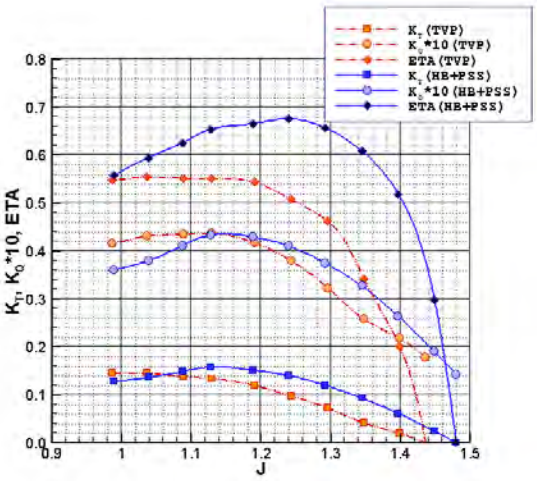

Fig. 24 The comparisons of performances of TVP2 and HB1 propeller with PSS at 36 knots and 10 degrees inclined shaft condition.

REFERENCES

Black, S. Shen, Y. and Stuart Jessup, S. (2006). "Advanced Blade Sections for High Speed Propellers", Carderock Division, Naval Surface Warfare Center, Bethesda, MD 20817.

Eppler, R. and Somers, D.M. (1980). "A Computer Program for the Design and Analysis of Low-Speed Aitfoils", Tech. Rep., NASA TM 80210

Giles, M. Drela, M. (1986). "A two-dimensional transonic aerodynamic design method," AIAA Journal, 25(9).

Henne, P.A. (1985). "An inverse transonic wing design method", AIAA paper 85-0330

Hsin, C.-Y. (1994). "Application of the panel method to the design of two-dimensional foil sections", J. of Chinese Society of Naval Architecture and Marine Engineers, 13(2), pp.1-11.

Hsin, C.-Y. and Chang, Y.-L. (1998). "Solving a Hydrodynamic Design Problem by a Distributed Computing System", Proceedings of the 3rd International Conference on Hydro-dynamics, Seoul Korea.

Hsin, C.-Y. and Chang, Y.-L. (2000). "A Hydrodynamic Design Method Developed on a Distributed Computing System", Transcations of the Aeronautical and Astronautical Society, 32(1), pp.89-95.

Hwang, J. L., Hsin, C. Y., Cheng, Y. H. and Chin, S. S.（2009）, "Design of Inflow-Adapted Foil Sections by Using a Multi-Objective Optimization Method", smp'09, Trondheim, Norway.

Hwang, J.L., Chin, S.S., Hsin, C.Y. and Chang, K.K. (2011), "Development of the Trans-Velocity Propellers", smp'11, Hamburg, Germany

Scherer, O. and Stairs, R., (1994). "Propeller Blade Sections with Improved Cavitation Performance", Propellers/Shafting '94 Symposium; 20-21 Sept 1994; Virginia Beach, VA, USA. Sponsored and Publ by SNAME, USA. Pprs. Ppr no 17

Shen, Y.T. (1996), "Dual-Cavitation Hydrofoil Structures," US Patent 5551369.

Young, Y.L. and Shen, Y.T. (2007), "A Numerical Tool for the Design/Analysis of Dual-Cavitating Propellers", Transactions of the ASME, Vol. 129.

Kehr, Y.Z., Liu, J.H., Li, Y.C., "Development of New Section Propeller in High Speed Craft", 13th SNAME, 2001, Taiwan.

Kerwin J.E. (1982), "Numerical Method for Propeller Design and Analysis in Steady Flow", Trans. SNAME, 1982